Science of the Total Environment 792 (2021) 148383

Contents lists available at ScienceDirect

Science of the Total Environment

journal homepage: www.elsevier.com/locate/scitotenv

Phosphorus cycling in freshwater lake sediments: Influence of seasonal water level fluctuations

Xiancang Wu, Teng Ma *, Yao Du, Qianqian Jiang, Shuai Shen, Wenhui Liu

School of Environmental Studies, China University of Geosciences, Wuhan 430074, China
State Key Laboratory of Biogeology and Environmental Geology, China University of Geosciences, Wuhan 430078, China

HIGHLIGHTS

- How water level fluctuation effects P cycle in freshwater lakes was examined.
- Water level rise enhanced suspended matter deposition and increase of Fe-P and Org-P.
- Fe-oxides reductive dissolution and organic matters degradation dominated P cycle.
- Conversion between Ca-P and Detr-P in individual seasons was found.
- Acidic dissolution of detrital apatite resulted in the increase of Ca-P.

GRAPHICAL ABSTRACT

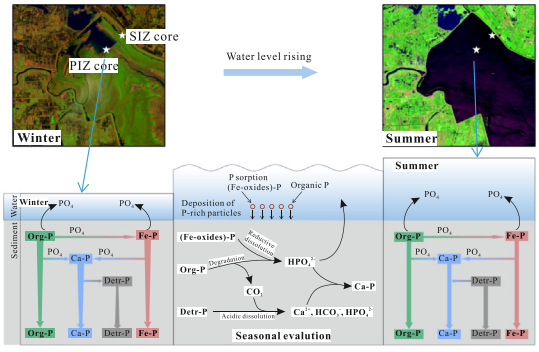

ARTICLE INFO

Article history:
Received 29 April 2021
Received in revised form 22 May 2021
Accepted 7 June 2021
Available online 10 June 2021

Editor: José Virgílio Cruz

Keywords:
Iron-associated P
Organic P
Apatite authigenesis
SEDEX
Seasonal evolution

ABSTRACT

Freshwater lakes experience drastic water level fluctuations because of climate change and human activities. However, the influence of such fluctuations on phosphorus cycling in sediments has rarely been investigated. We conducted a geochemical investigation on the phosphorus cycle in a shallow freshwater lake, Dongting Lake; under the influence of human activities and climate change, its water regime undergoes drastic changes. Irrespective of the permanent inundation zone (PIZ) or seasonal inundation zone (SIZ), the phosphorus cycle in sediments was found to be dominated by the reductive dissolution of iron (Fe) (oxyhydr)oxides, degradation of organic matters, and conversion between authigenic phosphorus (Ca-P) and detrital phosphorus in individual seasons. From winter to summer, with increasing water level, the content of Fe-bound phosphorus and organic phosphorus increase due to the deposition of suspended matter, thus increasing total phosphorus in PIZ. Moreover, the rising water level also reduces the dissolved oxygen content and promotes the reductive dissolution of Fe (oxyhydr)oxides. The mineralization of increased organic matter can release CO_2 and reduce pH in the vicinity, which can further result in the acidic dissolution of detrital apatite. In turn, most of the released phosphorus can be adsorbed or co-precipitated with calcium minerals, resulting in the significant increase of Ca-P. The mechanisms of phosphorus transformation in SIZ are similar to those in PIZ, but most of the increased organic matter and total P in a core from SIZ are attributable to the decomposition of plant matter. Therefore, the water level rise not only changes the conservative speciation of phosphorus in sediments to active speciation, but also triggers the release of phosphorus adsorbed to oxides and further increases the risk of phosphorus release from sediments to overlying water. Thus, our findings have major implications for freshwater shallow lakes and their P-driven productivity.

* Corresponding author at: School of Environmental Studies, China University of Geosciences, Jincheng Road 68, Wuhan 430078, China.
E-mail address: mateng@cug.edu.cn (T. Ma).

https://doi.org/10.1016/j.scitotenv.2021.148383
0048-9697/

1. Introduction

As an essential nutrient, phosphorus (P) controls the primary productivity and trophic status of freshwater lakes. In particular, sediment exchange—resuspension and flux of dissolved P across the sediment–water interface—plays a crucial role as internal P loading or potential P sink (McMahon and Read, 2013; Rothe et al., 2014). The mechanisms by which P is released or sequestered in sediments are strongly dependent on bottom water redox conditions, which are significantly influenced by water level. Understanding the impact of changes in bottom water oxygenation on the benthic P cycle is of great importance in light of the globally increasing lake water level fluctuations induced by the increasingly frequent occurrence of climate change events and human activities (Hu et al., 2018; Vanderkelen et al., 2018; Ye et al., 2013).

In aquatic systems, P speciation is dominated by particulate and colloidal fractions. Under oxic conditions, aquatic systems contain relatively low dissolved P content (Baken et al., 2016a; Van der Grift et al., 2018) because of the fast sorption kinetics of dissolved P on suspended matter (House, 2003). Suspended P may bind to Ca, Fe, Mn, and Al, either through adsorption onto particle surface or precipitation as a mineral. Moreover, organic P compounds are also associated with suspended P, which may be deposited on the surface of sediments or enter the sediment with water flow. The degradation of organic matter typically releases phosphate (denoted as HPO_4^{2-}) to the pore water, which is further sequestered by iron (Fe) (oxyhydr)oxides (henceforth termed Fe-oxides) in surface sediments (Li et al., 2018; Slomp et al., 1996). The Fe-bound P is released back to the pore water during sediment burial as Fe-oxides undergo reductive dissolution. Subsequently, the dissolved HPO_4^{2-} can precipitate as authigenic P minerals in sediments or diffuse back to the sediment surface, where it typically is either adsorbed or escapes to the overlying water (Dijkstra et al., 2018; Markovic et al., 2019; Xiong et al., 2019). Accordingly, the biogeochemical cycle of P is strongly dependent on redox conditions.

The authigenesis of Fe phosphates is also important in sedimentary P sequestration. In some sediments, Fe^{2+} released by the reductive dissolution of Fe-oxides are not entirely transferred to dissolved sulfides (HS^-) to form Fe-sulfides, leading to the subsequent precipitation of the remaining Fe^{2+} with phosphates to form the Fe(II)-phosphate phase such as vivianite ($Fe_3(PO_4)_2$) after the complete consumption of HS^- (Egger et al., 2015; Rothe et al., 2016). Lacustrine sediments, which are naturally rich in Fe-oxides and coupled with low SO_4^{2-} concentration, thus provide ideal conditions for vivianite authigenesis (Gachter and Muller, 2003; O'Connell et al., 2015; Rothe et al., 2014). Although direct mineralogical identification of vivianite in sediments is difficult because of its low concentrations, fine granularity, and potentially poorly crystalline nature, previous studies have suggested the significant relevance of vivianite formation in P sequestration (Egger et al., 2015; Rothe et al., 2014; Xiong et al., 2019). However, in the presence of HS^-, Fe^{2+} tends to precipitate as Fe-sulfides rather than Fe-phosphates. Consequently, the balance between HS^- and Fe^{2+} released into the pore water dominates the fate of dissolved HPO_4^{2-} in sediments (Rothe et al., 2016).

In addition to Fe-S-P systematics, the calcium–P phases (such as biogenic hydroxyapatites and detrital apatite) are also considered as stable end products of P diagenesis and constitute the long-term P burial phase (Anderson et al., 2001; Kraal et al., 2017). In lake water, pH changes driven by photosynthesis can result in the precipitation of P and calcite. This particulate P phase is less sensitive to the dissolved HS^- than Fe-P and inorganic polyphosphates, and is eventually deposited on sediments (House, 2003; Reddy et al., 1999). However, the formation and conversion mechanisms of calcium–P phases in sediments are not completely understood. Previous studies have reported that low availability of organic matter and high alkalinity can limit the formation of authigenic Ca-P (Kraal et al., 2010; Schenau et al., 2000). Under anoxic conditions, limited formation of carbonate fluorapatite and extensive formation of apatite have been reported (Kraal et al., 2012; Kraal et al., 2015; Schenau et al., 2000). Moreover, the reductive dissolution of Fe-oxides can result in a shift from Fe(III)-bound P to P adsorbed onto $CaCO_3$, while the oxidation of organic and pyritic matter can cause the acidic dissolution of detrital apatite, which has been considered a conservative P phase, and further to the formation of Fe-bound P and authigenic Ca-P (Filippelli, 2002; Kraal and Slomp, 2014; Kraal et al., 2017). Therefore, the calcium–P phases are most likely promoted by organic matter content.

With the increase of extreme weather events and human activities, lake water level fluctuations are becoming increasingly more prominent. The seasonal rise and fall of water level directly affects the redox conditions of lake bottom sediments, deposition of suspended particles, and types and survival of benthic organisms and microorganisms (Carmignani and Roy, 2017; Lécrivain et al., 2021; Ren et al., 2019; Wu et al., 2020a), which in turn have important effects on the P cycle. Although the dynamics of P in lake water and sediments have been investigated (Coppens et al., 2016; Hambright et al., 2004; Tang et al., 2018), the seasonal geochemical characteristics of P speciation remain poorly understood. As the second largest freshwater lake in China, Dongting Lake has been significantly influenced by the construction of the Three Gorges Dam (TGD) and climate change, leading to dramatic changes in its water regime and wide seasonal water level fluctuations (Feng et al., 2013; Yu et al., 2018; Yuan et al., 2015). Moreover, total phosphorus (TP) in lake sediments have been gradually increasing in Dongting Lake (Zhu and Yang, 2018), and sediments are an important internal P source for the lake water (Liang et al., 2017). With these conditions, Dongting Lake is an ideal site for studying the influence of water level fluctuations on the geochemical cycling of P speciation.

In this study, we investigated seasonal changes in different parts of Dongting Lake, including the permanent inundation zone (PIZ) and seasonal inundation zone (SIZ), to assess the seasonal changes of P recycling and the role of water fluctuation. Detailed investigations of the water column, pore water, and sediment chemical characterization were conducted in combination with the sequential extraction of P and Fe speciation. We highlight the influence of water level fluctuations on the acidic dissolution of detrital apatite and the potential risk of P release from sediments.

2. Methods and materials

2.1. Sample location and geological setting

As the second largest freshwater lake in China, Dongting Lake plays a critical role in flood regulation and storage capacity in the middle and lower reaches of the Yangtze River. This lake is actually composed of a series of lakes, with three major regions named Eastern, Southern, and Western Dongting Lake (Fig. 1). In recent years, the TP in both lake water and sediments has increased (Tian et al., 2017; Zhu and Yang, 2018). The highest TP (0.159 mg/L) has been recorded in East Dongting Lake (Tian et al., 2017), which consequently experiences light eutrophication. Due to the impoundment of TGD and climate change, the inundation area of Dongting Lake has decreased by approximately 17% (195.1 km^2) since 2003, resulting in earlier onset of the dry season and wide water level fluctuations ranging from approximately 20 m to approximately 34 m (Fig. S1) (data from Chenglingji Hydrological Station, CHS, http://yzt.hnswkcj.com:9090/#/) (Feng et al., 2013; Yuan et al., 2015).

The northwest of East Dongting Lake is the core area of the National Wetland Reserve and is less affected by human activities. Accordingly, this area was selected as the sampling area. Two main sampling points were set, including the PIZ core in the center of the lake and the SIZ core on the riparian zone (Fig. 1). The water depth of PIZ is approximately 0.5–7.5 m, while SIZ is submerged from July to August with a maximum water depth of approximately 5.5 m; it remains exposed in the other months. Fig. 1 clearly shows the rise of water level at the

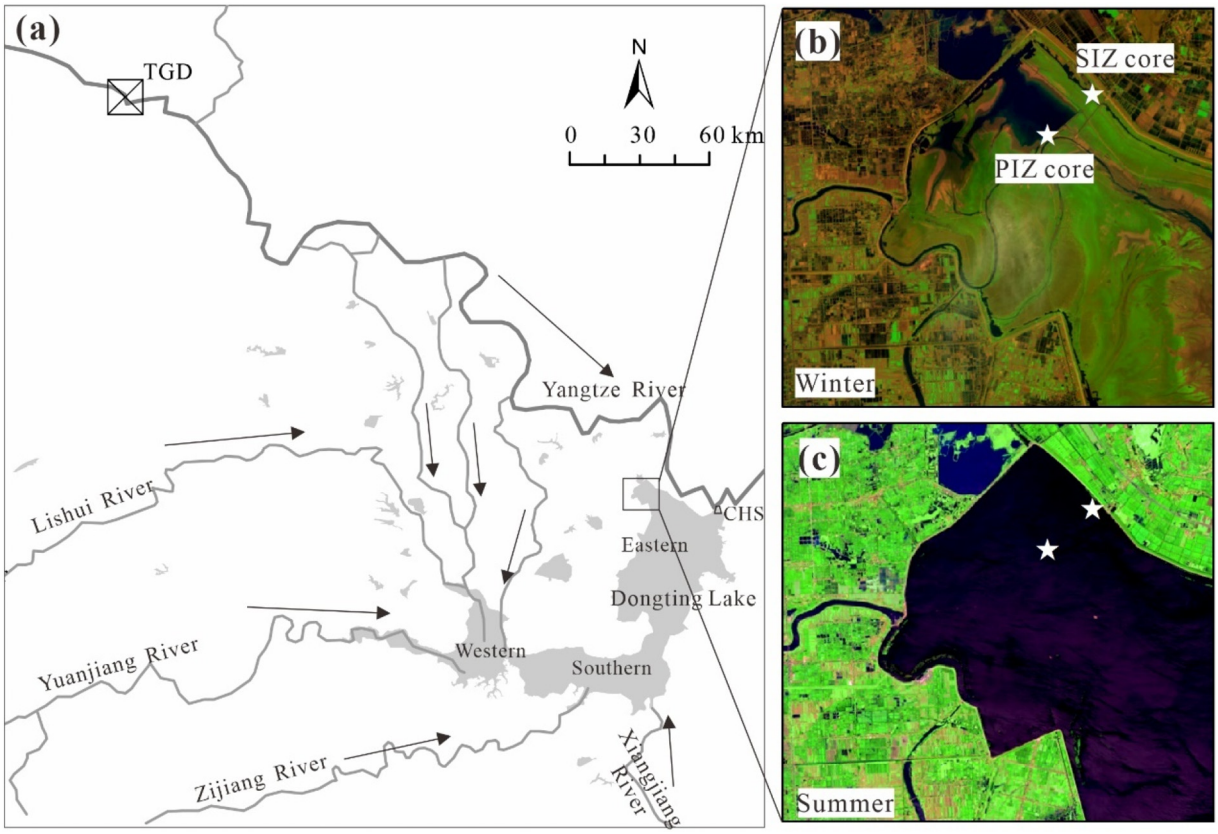

Fig. 1. Location of the study area and sampling sites. (a) Dongting Lake and its tributaries (The arrows show the flow direction of the rivers). Sampling sites in (b) winter and (c) summer. The false color remote sensing images of (b) and (c) for December 14, 2019 and August 26, 2020, respectively, were obtained from USGS Landsat 8 sensors (https://glovis.usgs.gov/).

sampling sites, which are characterized by fine-grained sediments and sediment accumulation rates of approximately 1.18–1.28 cm yr^{-1} (Chen et al., 2016; Du et al., 2001).

2.2. Water column, pore water and sediment sampling

Sampling was conducted in winter (January 2020) and summer (September 2020). Sediment samples, water column samples, and pore water samples were collected from a core in each sampling period. All water column samples were collected from the sediment–water interface using a 5 L polymethyl methacrylate sampler, which was rinsed three times before sampling. Water samples were filtered through a 0.45 μm nylon filter and stored in pre-cleaned polythene bottles at 4 °C until analysis for total dissolved P (TDP), SO_4^{2-}, Cl^-, HCO_3^-, TFe, K^+, Mg^{2+}, Ca^{2+}, and Na^+, while the samples for TP analysis were not filtered.

Sediment core samples (up to 30 cm) were taken from both cores using a Universal Percussion Corer, Aquatic Research Instruments (http://www.aquaticresearch.com/universal_core_head.htm), and the schematic diagram of sediment core sample was showed in Fig. S2. After sampling, the cores were stored upright in the polycarbonate core barrel and refrigerated at 4 °C prior to processing, which was performed within 5 h. Sediment cores were sliced (generally in a thickness of 2 cm) in a N_2 filled glove bag using an Incremental Core Extruding Apparatus, Aquatic Research Instruments (http://www.aquaticresearch.com/core_extruding_apparatus.htm), and placed in 100 mL centrifuge tubes. For each slice, a sub-sample was collected in a pre-weighed aluminum box for water content analysis. Further, these samples were dried at 60 °C until the weight stabilized, and the water content was determined from the weight loss.

Pore water was extracted by centrifuging at 4000 rpm for 10 min from the second sub-sample in the glove bag. Pore water was stored in pre-cleaned polythene bottles at 4 °C for further analysis. However, because of the low water content, pore water could not be extracted from SIZ core sediment samples in winter. Sediment samples were immediately frozen after opening the glove bag, and subsequently freeze-dried and stored frozen in an anoxic chamber prior to analysis.

2.3. Water column and pore water analysis

Immediately after collection, pH, Eh, dissolved oxygen (DO), and temperature were measured with a multi-parameter portable meter (HACH HQ40D, USA). The concentrations of TDP, TFe, K^+, Mg^{2+}, Ca^{2+}, and Na^+ were determined by inductively coupled plasma optical emission spectroscopy (ICP-OES, PerkinElmer, Avio 200); HCO_3^- was measured by acid-base titration; Cl^- and SO_4^{2-} were determined by ion chromatography (ICS-1100, Thermo Fisher Scientific, USA), and the total analysis error was less than 5%. TP was analyzed by the molybdate blue method on a UV-1800PC spectrophotometer (AOE Instruments (Shanghai)) at 700 nm wavelength after digestion with potassium persulfate in an autoclave (120 °C, 0.5 h).

2.4. Sediment analysis

Before analysis, all the sediment samples were freeze-dried, powdered, grounded and sieved through a 75 μm sieve in a N_2 filled glove bag.

2.4.1. Total elemental composition

Total sulfur (TS), total carbon (TC), and total organic carbon (TOC) were analyzed with an elemental analyzer (vario EL cube, Elementar). TOC samples were pre-treated using 1 M hydrochloric acid (HCl) to remove carbonate phases. The relative standard deviation (RSD) of replicate analyses of TC, TOC, and TS was ≤5%. Total inorganic carbon (TIC)

was estimated as TIC = TC − TOC, and the RSD of replicate TIC analyses was ≤5%.

A split of approximately 100 mg of sediments was dissolved in 1.6 mL 6 M HNO_3 in a closed Teflon bomb at 120 °C for 30 min. Thereafter, 0.8 mL $HClO_4$ (70%) and 1.2 mL HF (40%) were added and heated to 150 °C for 180 min. The acids were then evaporated at 190 °C for 120 min and the resulting gel was subsequently dissolved in aqua regia, and finally evaporated to dryness at 120 °C. Total elemental contents were measured using ICP-OES. TP was obtained using the molybdate blue method as described above. The RSD of replicate sediment sample analyses was <6% for TP, Fe, Al and Ca, and the recoveries of replicate analyses of certified standards (GSD-9) set by the Institute of Geophysical and Geochemical Exploration (China) were 98%, 108%, 98%, and 97% for TP, Fe, Ca, and Al, respectively.

2.4.2. Sediment P extractions

The sequential extraction (SEDEX) method for different phosphorus phases was applied following Ruttenberg (1992), as modified by Zhang et al. (2010), Xiong et al. (2019) and Tao et al. (2020). Aliquots of 0.1 g dried sediment were subjected to the SEDEX method as follows: (i) exchangeable-P (Ex-P, extracted by 1 M $MgCl_2$, pH 8, 2 h), (ii) Fe-oxide bound P (Fe-P, extracted by sodium bicarbonate-dithionite solution (BD), pH 7, 8 h, followed by 1 M $MgCl_2$, pH 8, 2 h), (iii) authigenic Ca-P (Ca-P, including biogenic hydroxyapatite, $CaCO_3$-bound P and carbonate fluorapatite, extracted by Na-acetate buffer, pH 4, 6 h, followed by 1 M $MgCl_2$, pH 8, 2 h, 2 times), (iv) detrital Ca-P (Detr-P, mainly fluorapatite (FAP), extracted by 10% HCl, 16 h), and (v) organic P (Org-P, calculated by TP minus the sum of the above four inorganic speciation). All P phases were analyzed using the method described above. Measured concentrations from duplicate analysis deviated by less than 7%.

Reactive P ($P_{reactive}$) was determined as: $P_{reactive}$ = Ex-P + Fe-P + Ca–P + Org-P.

2.4.3. Sediment Fe extractions

The method of extracting Fe phases was adopted from Canfield et al. (1986) and Poulton and Canfield (2005), as modified by Goldberg et al. (2012) and Xiong et al. (2019). Overall, the procedure targets six operationally defined phases with five steps; steps I–III were performed sequentially.

To investigate the solid-phase partitioning of Fe, a second 0.1 g aliquot of dried sediment was subjected to the extraction procedure for Fe. The samples were initially treated with 0.5 M HCl for 1 h. The Fe extracted by this step includes poorly crystalline ferric (oxyhydr)oxides such as ferrihydrite, in addition to any unsulfidized Fe(II) produced during early diagenesis (either by reaction with dissolved sulfide or by dissimilatory Fe reduction), which was either not fully released to solution or was re-adsorbed to particle surfaces. Fe(II) released by the 0.5 M HCl extraction (termed as $Fe(II)_{HCl}$) was determined immediately by the ferrozine method (Stookey, 1970) on an aliquot of the solution. Highly reducible ferric oxides (Fe_{ox1}) were obtained through the subtraction of the measured $Fe(II)_{HCl}$ from the total Fe present in the 0.5 M HCl extract. In the next step, a sodium citrate-acetic acid-sodium dithionite solution kept at pH 4.8 for 2 h was used to extract crystalline Fe-oxides (such as hematite and goethite, termed Fe_{ox2}), after which ammonium oxalate-oxalic acid was extracted for 6 h to dissolve magnetite (Fe_{mag}). The total Fe released in each extraction was measured using the ferrozine method. Measured concentrations from duplicate analyses deviated by <8%.

Sulfide-bound Fe phases, as pyrite (Fe_{py}) and acid-volatile sulfur (Fe_{AVS}), were extracted using the technique of Canfield et al. (1986), as simplified by Burton et al. (2008). A third 10.0 g aliquot of dried sediment was used to sequentially determine the amount of Fe_{AVS} (using 6 M HCl) and Fe_{py} (using an acidic chromous chloride solution) via the diffusion-based approach described by Burton et al. (2008) using iodometric titration of the alkaline Zn-acetate trap. Measured concentrations from duplicate sample extractions varied by <8% for Fe_{py} and <7% for Fe_{AVS}.

2.5. Data analysis

The saturation indexes (SI) of porewater were calculated using PHREEQC Interactive 3.2.0. Minerals with SI values greater than 0, equal to 0, and less than 0 correspond to oversaturation with a tendency to precipitate, equilibrium with the solution, and undersaturation with a tendency to dissolve if present, respectively.

Inverse modeling is used to examine the molar transfer of minerals and gases, which explains the compositional differences between the initial and final waters within a specified range of uncertainties. The object of inverse modeling is to find sets of minerals and gases that, when reacted in appropriate amounts, account for differences in composition between two solutions. In this study, inverse modeling was also performed using PHREEQC Interactive 3.2.0.

To identify the relationship among variations in phosphorus speciation from winter to summer, correlation analysis was performed. The Spearman R correlation was calculated using SPSS 22, because the components do not satisfy the standard normal distribution.

3. Results

3.1. Water content of sediments

The water content of the core collected from PIZ in winter exhibited a progressive decrease with depth (Fig. 2), from approximately 60% wet weight at the sediment surface to approximately 26% wet weight at 28 cm. In contrast, the water content was higher in summer than in winter. It also exhibited a decrease with depth, with values from 72% to 39% wet weight. In the SIZ core, similar declines in the water content with depth were observed in both seasons, with values decreasing from approximately 44% to 32% wet weight and 75% to 58% wet weight during winter and summer, respectively. The significant increase of water content in both cores from winter to summer indicates water level rise.

3.2. Water column hydrochemistry

Overall, the concentrations of almost all lake water components were higher in winter than in summer, leading to a high EC in winter (Table 1). This may be attributable to the recharge by tributaries in summer and heavy rainfall, which dilute the lake water significantly.

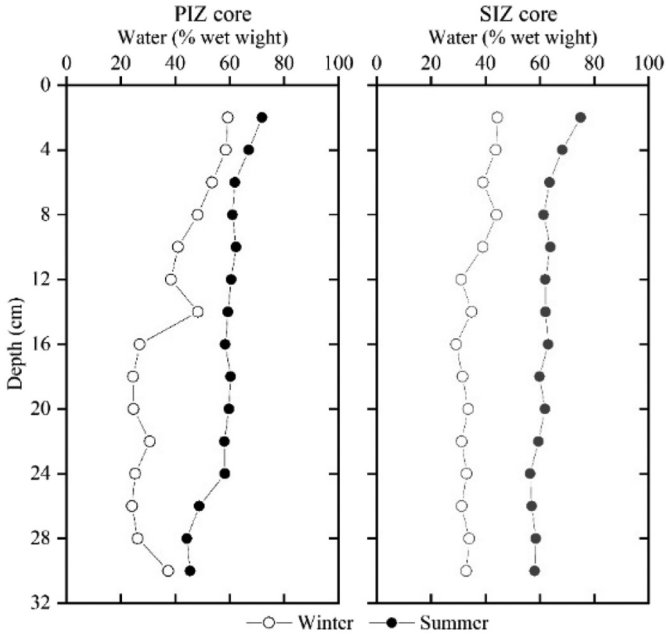

Fig. 2. Water content profiles.

Table 1
Hydrogeochemical parameters of the water column.

Sample Id	Sampling time	Water depth (m)	T (°C)	pH	EC (μS/cm)	Eh (mV)	DO (mg/L)	Fe (mg/L)	Ca (mg/L)	Mg (mg/L)	Al (μg/L)	TDP (mg/L)	HCO_3 (mg/L)	SO_4^{2-} (mg/L)	TP (mg/L)	DOC (mg/L)
PIZ	Summer	7.4	28.7	7.84	313	43.5	3.41	0.01	49.05	9.75	13.71	0.032	150	28.01	0.058	7.69
	Winter	0.5	10.1	8.35	384	140.9	11.89	0.02	54.63	12.31	34.56	0.051	145	49.00	0.186	59.09
SIZ	Summer	5.6	28.1	7.75	315	59.8	3.74	0.02	49.62	9.57	10.02	0.052	150	29.53	0.041	21.92

The temperature of the lake water was 10 °C in winter and 28.1–28.7 °C in summer (Table 1). The pH of the overlying water was slightly higher in winter. The DO concentration and Eh of the water were clearly higher in winter than in summer, which can be explained by the shallower water depth in winter; the DO content in winter was approximately 3.5 times that in summer. The content of dissolved Fe in surface water was very low because of the high Eh in both seasons. In summer, the TDP and TOC contents of PIZ water samples were significantly lower than those of SIZ samples, while the TP content of PIZ was slightly higher than that of SIZ (Table 1). These differences can be explained by the herbaceous plants growing in SIZ in the dry season, which decay after being submerged in the wet season, increasing the organic matter content.

3.3. Pore water hydrochemistry

3.3.1. PIZ

The concentration of Fe^{2+} remained relatively low and stable with values ranging from 0.5 μM to 2.8 μM in winter, but it exhibited a significant fluctuation ranging from 0.7 μM to 31 μM in summer (Fig. 3). Fe^{2+} concentration was somewhat higher at depths below 10 cm than above 10 cm due to the decrease of DO. The concentration of PO_4^{3-} exhibited a progressive decrease with depth in winter, from approximately 10 μM at the sediment–water surface to approximately 0.12 μM at 14 cm (Fig. 3). In summer, PO_4^{3-} and Fe^{2+} concentrations were similar, with considerable variations and higher values below 10 cm. SO_4^{2-} concentration decreased from 162 μM at the surface to 30 μM at 12 cm, followed by an increase to approximately 85 μM at 26 cm. In winter, SO_4^{2-} concentration exhibited a progressive increase with depth from approximately 573 μM to 1280 μM, and the values were much higher than that in summer. This is possibly attributable to the deeper water level in summer, which further leads to a more reductive environment in sediments. HCO_3^- increased from approximately 3.6 mM to 8.3 mM at the upper 14 cm, followed by a drop to approximately 6.5 mM at 26 cm in summer. In contrast, HCO_3^- concentration exhibited a progressive decrease in winter. Ca^{2+} concentration showed similar changes with HCO_3^- in both seasons, indicating a balance in the dissolution/precipitation of various types of calcium minerals.

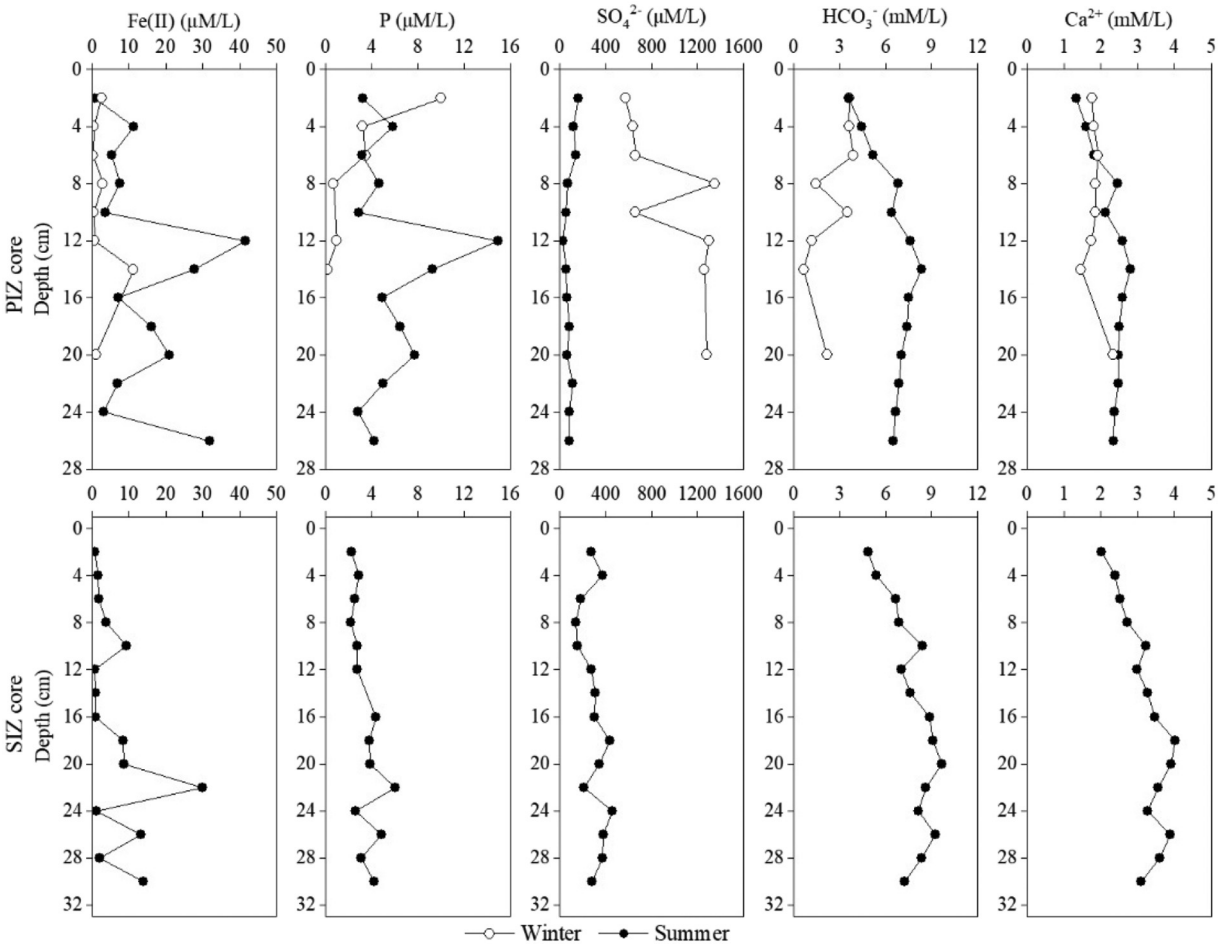

Fig. 3. Porewater depth profiles and seasonal comparisons between January and September for dissolved Fe^{2+}, PO_4^{3-}, SO_4^{2-}, HCO_3^- and Ca^{2+} concentrations with depth.

3.3.2. SIZ core

Because of low water content, pore water samples could not be collected from SIZ in winter. In summer, Fe^{2+}, PO_4^{3-}, and SO_4^{2-} concentrations in SIZ and PIZ showed similar profiles (Fig. 3). Fe^{2+} concentration increased slightly with depth but it remained low. Similarly, PO_4^{3-} content also increased progressively with depth. SO_4^{2-} concentration showed a relatively wide fluctuation with values ranging from approximately 140 μM to 380 μM. HCO_3^- increased from approximately 4.8 mM to 20 mM at the upper 14 cm, and subsequently decreased to approximately 7.2 mM at 30 cm. Ca^{2+} concentration was also similar to HCO_3^- concentration.

3.4. Sediment geochemical composition

3.4.1. Bulk composition

3.4.1.1. PIZ core. TIC content initially decreased from 2% to 0.88% in the upper interval up to a depth of 16 cm, and then increased to 1.4% at 24 cm and subsequently dropped to 0.88% at 30 cm in winter (Fig. 4). In summer, TIC content was relatively high throughout the core. The concentration of TOC was stable in the upper 12 cm, with values of approximately 17%, and subsequently decreased to approximately 6% due to microbial remineralization in winter. In summer, TOC concentration slightly decreased without any significant variation, from approximately 18% in the sediment–water interface to 15% at 30 cm.

TS concentration remained stable in summer, with values of 0.27–0.29% (Fig. 4). In winter, it sharply decreased with depth at the upper 18 cm, from approximately 0.6% at the sediment–water surface to approximately 0.28% at 18 cm. Below 18 cm, it remained relatively stable. Overall, TS concentration was relatively high throughout the core in winter. Bulk P content decreased slightly with depth in winter, from 870 μg/g to 750 μg/g. In summer, TP concentration remained stable in summer with values of approximately 900 μg/g (Fig. 4); it was relatively high throughout the core. In winter, TFe concentration first increased slightly, then decreased to the lowest value of 45 mg/g, and finally increased to approximately 70 mg/g. TFe concentrations in summer and winter were similar, and remained high.

The concentrations of Ca and Al showed similar trends in both seasons (Fig. 4). The concentration of Ca decreased slightly with depth, while detrital elements (Al) remained stable. Nevertheless, the concentrations of Ca and Al in winter were somewhat lower than those in summer.

3.4.1.2. SIZ core. The concentration of TIC significantly fluctuated in the SIZ core (Fig. 4). In winter, TOC concentration slightly increased at the upper 8 cm, followed by a sharp decrease due to mineralization, but it exhibited a stable profile in summer. However, TOC concentrations generally remained above 0.8% below 14 cm in winter. Both TIC and TOC concentrations were higher in summer than in winter.

TS remained stable in both seasons, with overall slight decreases with depth from 0.33% to 0.27% in summer and 0.39% to 0.22% in winter (Fig. 4). P concentration also exhibited a stable profile in summer with values of 950 μg/g, but it showed a slight decrease with depth in winter, with values dropping from approximately 1055 μg/g to approximately 850 μg/g.

The concentrations of TFe, Ca, and Al fluctuated significantly in both seasons (Fig. 4). In contrast, the concentrations of TFe and Al were similar in both seasons, fluctuating between 48 mg/g and 66 mg/g for TFe and 69 mg/g and 89 mg/g for Al. Ca concentration was somewhat higher in summer than in winter.

3.4.2. Iron speciation

3.4.2.1. PIZ core. $Fe(II)_{HCl}$ concentrations were relatively low and showed increases with depth throughout the profile to approximately 6 mg/g (Fig. 5). The highly reducible Fe oxide pool (Fe_{ox1}) was also low and decreased slightly with depth. In contrast, the more crystalline Fe (oxyhydr)oxides (Fe_{ox2}) were more abundant and remained relatively constant at the upper 26 cm, followed by a significant increase below 26 cm in winter; it was more stable in summer. Fe_{mag} is a minor

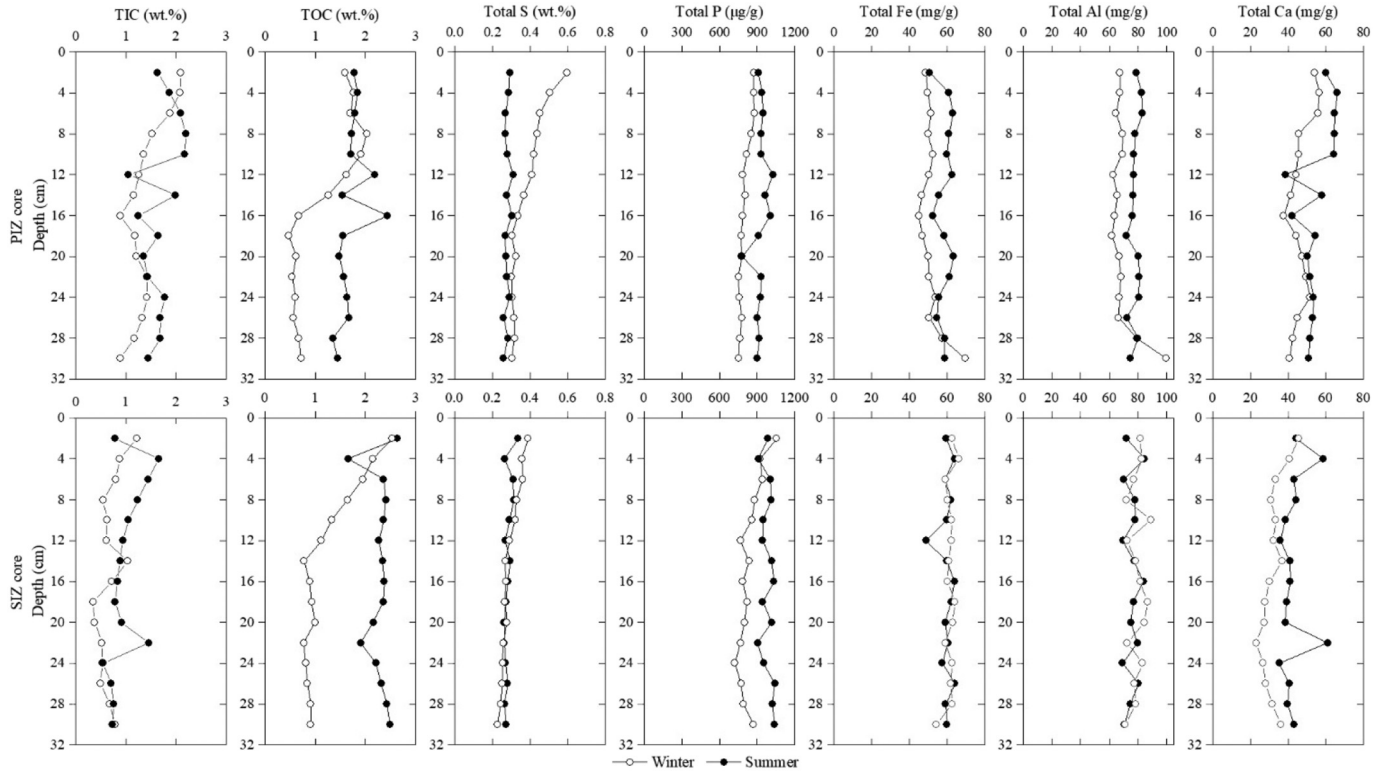

Fig. 4. Solid phase sediment profiles of TIC, TOC, TS, P, Fe, Al, and Ca in different seasons.

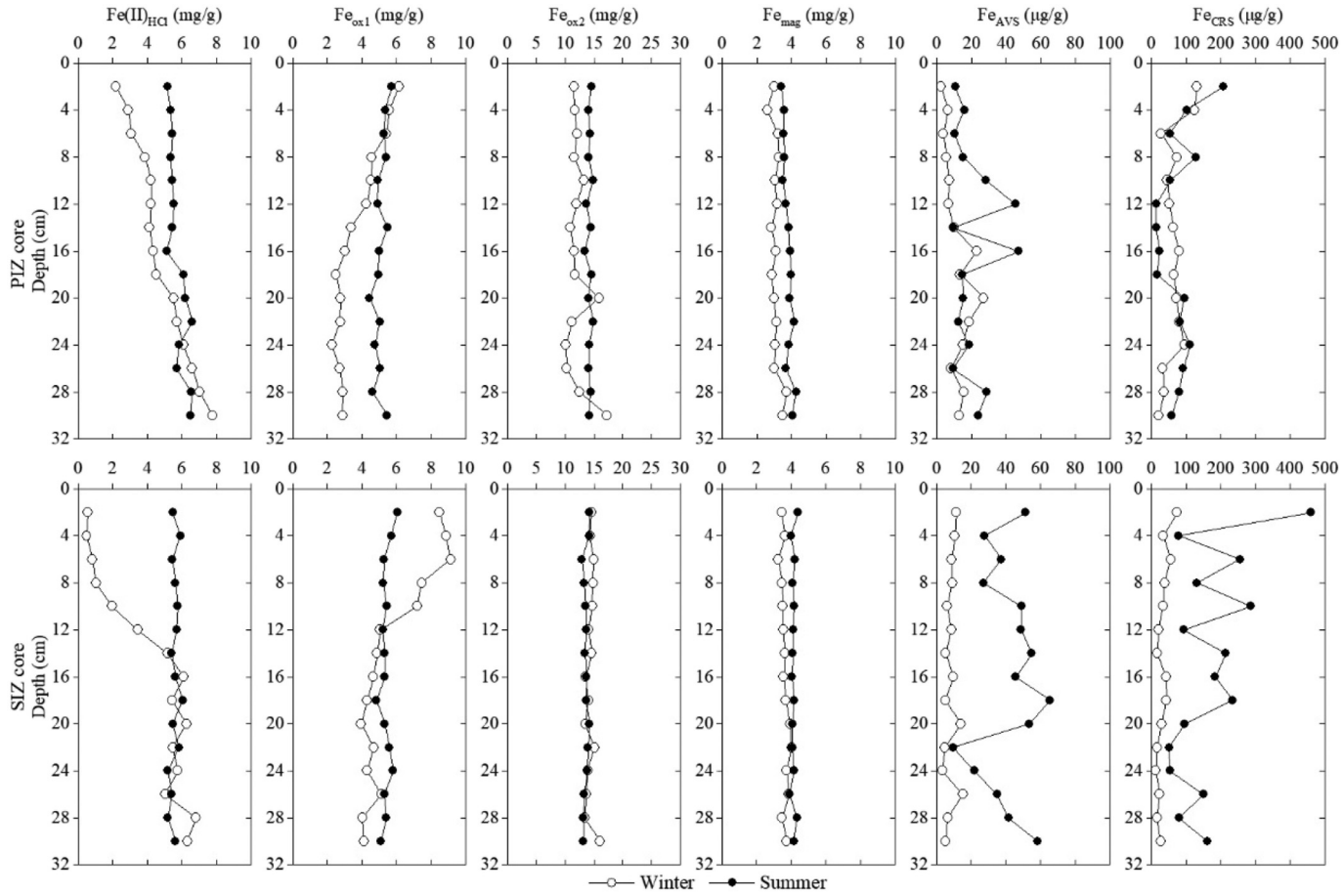

Fig. 5. Iron speciation profiles for the two cores in different seasons.

constituent and also remained relatively constant in both seasons. The concentrations of $Fe(II)_{HCl}$, Fe_{ox1}, Fe_{ox2}, and Fe_{mag} were somewhat higher in summer than in winter (Fig. 5).

Fe_{AVS} and Fe_{py} showed relatively low concentrations in both seasons (Fig. 5). Fe_{AVS} concentration fluctuated significantly in summer, with a progressive increase from 9.2 μg/g to 47.2 μg/g at the upper 16 cm, while in winter, Fe_{AVS} increased gradually from 2.3 μg/g to 27.0 μg/g at the upper 22 cm. The concentrations of Fe_{py} showed a similar progressive decline with depth in both seasons, with similar values.

3.4.2.2. SIZ core. In winter, $Fe(II)_{HCl}$ concentrations were very low at the upper 8 cm and increased to approximately 6 mg/g at 16 cm, below which it became relatively stable. In summer, $Fe(II)_{HCl}$ was more stable at approximately 6 mg/g (Fig. 5). The concentrations of Fe_{ox2} decreased with depth in both seasons. Fe_{ox2} and Fe_{mag} remained relatively constant throughout the core in both seasons. Remarkably, these four species of Fe remained largely the same below 14 cm in both seasons.

The concentrations of Fe_{AVS} and Fe_{py} were also very low in the SIZ core in both seasons (Fig. 5). In winter, Fe_{AVS} and Fe_{py} showed a decrease throughout the core. However, in summer, the concentrations of both Fe_{AVS} and Fe_{py} varied considerably, from 9.5 μg/g to 65.4 μg/g for Fe_{AVS} and 50.1 μg/g to 460.1 μg/g for Fe_{py}.

3.4.3. Phosphorus speciation

3.4.3.1. PIZ core. The concentration of loosely bound P (Ex-P) was very low and remained relatively stable in both seasons (Fig. 6). In winter, the concentration of Fe-associated P (Fe-P) decreased up to a depth of 16 cm, and then progressively increased below 26 cm. Fe-P exhibited a more stable profile in summer, with an overall slight decrease with depth. The content of authigenic carbonate fluorapatite (Ca-P) remained relatively constant with depth in summer, but it slightly decreased in winter (Fig. 6). Detr-P also remained stable in summer, but slightly decreased at the upper 10 cm, and then progressively increased in the 12–26 cm interval, after which it decreased. The concentration of organic-bound P (Org-P) varied considerably with a trend of initial decline and subsequent rise in winter. Org-P was more stable in summer, except at one sampling point. Except for Detr-P, the concentrations of the other four P species significantly increased from winter to summer.

3.4.3.2. SIZ core. Ex-P and Fe-P concentrations were similar between the SIZ and PIZ cores (Fig. 6). In SIZ, Ex-P was very low and remained stable but Fe-P was somewhat higher. Ca-P and Detr-P fluctuated significantly in winter, but they were more stable in summer. Org-P varied considerably in both seasons.

4. Discussion

4.1. Water geochemistry evolution from winter to summer

The most significant change in lake water is the rise of the water level from winter to summer, which can not only alter the chemical composition of lake water, but also enhance the mixing of lake water and pore water, and even change the pore structure of sediments.

The lake water depth increased from approximately 0.5 m in winter to 7.5 m in summer for PIZ and from 0.0 m in winter to approximately 5.5 m in summer for SIZ. The increase of water in Dongting Lake is mainly attributable to rainfall and recharge from tributaries (Hu et al., 2018; Yu et al., 2018). The rise of the water level can weaken the contact between sediments and air, thus inducing a reducing environment for

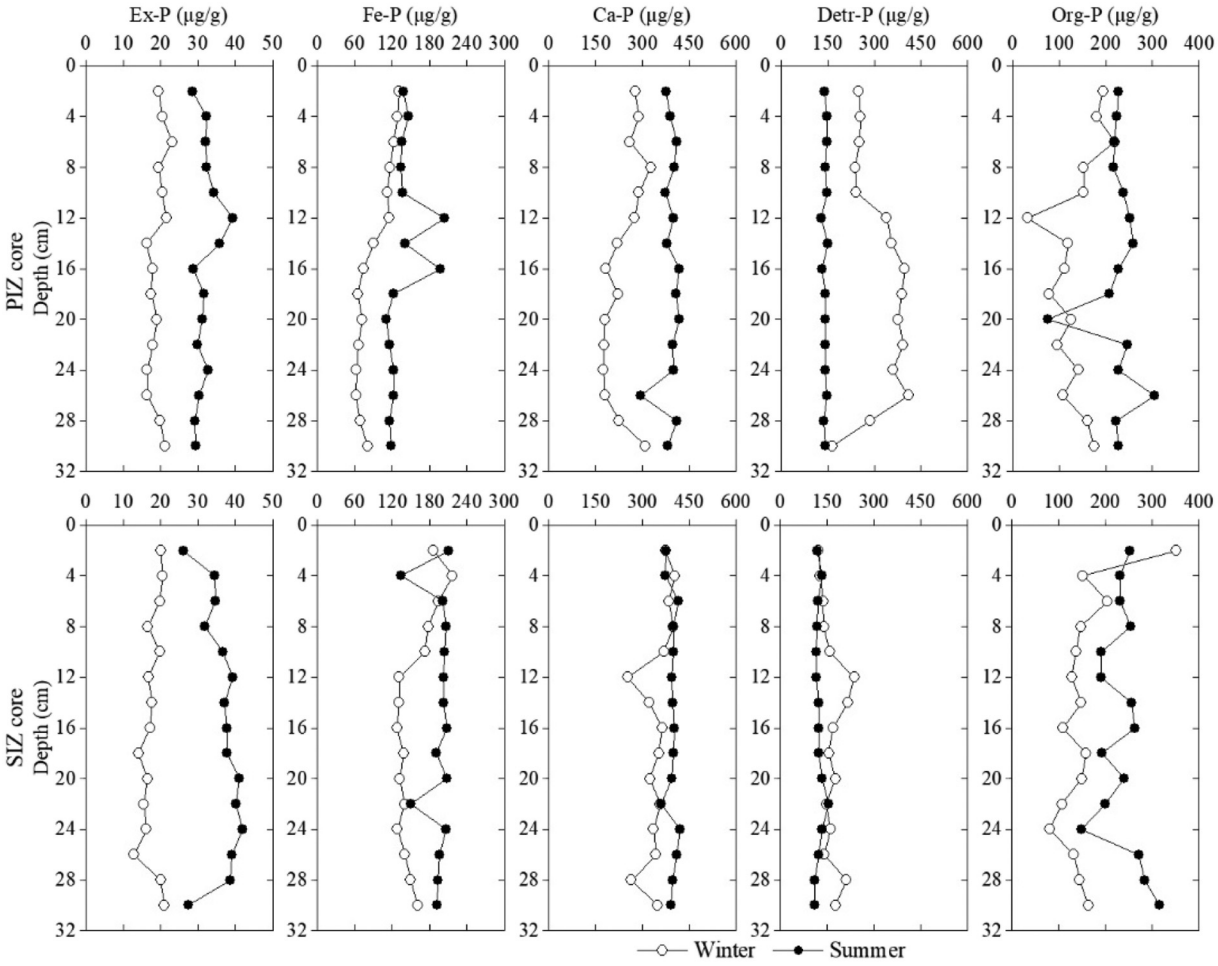

Fig. 6. P speciation profiles for the two cores in different seasons.

the sediments. The hydraulic gradient between lake water and sediment pore water will also increase, which promotes the introduction of lake water into sediment pores. Consequently, the chemical characteristics of pore water become similar to those of lake water. Because of its conservative chemical properties, Cl^- is often used as an indicator of mixing between different water bodies (Wu et al., 2020a; Yuan et al., 2020). It is clearly shown in Fig. S3 that the Cl^- content of pore water is basically the same as that of lake water in both PIZ and SIZ, which suggests increased recharge of pore water by lake water in summer. This is also indicated by the increase in the water content of sediments (Fig. 2). Further, the increase of the water depth and amount of lake water infiltration can also reduce the redox gradient of pore water, which is consistent with the more stable concentrations of SO_4^{2-} and $Fe(II)_{HCl}$ in summer (Figs. 3 and 5).

Moreover, due to the heavy rainfall and faster flow of surface water in summer, more particulate matter will enter the lake (Zheng et al., 2015). In the lake center (PIZ), the water body tends to be static, which is conducive to the deposition of particulate matter. This part of particulate matter can enter sediment pores with lake water and further accumulate. These increased deposits will effectively increase the contents of Fe, Al, and organic matter in sediments (Fig. 4). The deposition of fine particulate matter has also been investigated in other studies (Cui et al., 2021; Nivala et al., 2012; Ulrich et al., 2015). In the lake riparian zone (SIZ), the water flow is faster and not conducive to the deposition of suspended matter. Consequently, the contents of Al in SIZ remain stable in both winter and summer (Fig. 4). However, the content of TOC is higher in summer than winter, which may be attributable to the decomposition of herbaceous plants that flourish in SIZ in winter.

The pore water chemistry data show several prominent features of importance to this study. In the PIZ core, the concentration of SO_4^{2-} was much lower in summer than in winter, which is consistent with the lower TS content in sediments in summer. The lower concentration should not be attributed solely to the mixing of lake water. If only the mixing of lake water is considered, the concentration should be about 300 μM. However, the actual concentration was below 162 μM and decreased with depth, suggesting a sulfate reduction nature of sediments in the PIZ core in summer (Su et al., 2018). The similar increase of Fe^{2+} and PO_4^{3-} concentration from winter to summer in the PIZ core (Fig. 3) might be a consequence of phosphate release from the reduction of Fe-oxides, which is considered in more detail below.

However, in SIZ, the SO_4^{2-} content in pore water was somewhat higher than that in lake water, which suggests that SIZ has a more oxidative environment than PIZ in summer. Ca^{2+} and HCO_3^- showed a similar trend in both PIZ and SIZ, indicating an equilibrium in the dissolution/precipitation of carbonate minerals (Wu et al., 2020b).

4.2. Iron geochemical characteristics

In the center of the lake, the dissolved oxygen content of lake water was high in winter (11.89 mg/L), which led to the low $Fe(II)_{HCl}$ concentration in the sediment surface in PIZ. With increasing depth, the most reactive Fe_{ox1} minerals are initially reduced, and thus this phase decreases significantly with depth in the PIZ core in winter, whereas the more crystalline Fe-oxides comprising the Fe_{ox2} pool react more slowly and persist with depth (Fig. 5) (Canfield, 1989; Poulton et al., 2004). After dissolution, the produced Fe(II) can react with dissolved sulfide

to form Fe_{AVS} and ultimately pyrite (Flores-Alsina et al., 2016; Xiong et al., 2019), or react with phosphorus to form ferrous phosphate minerals, which are discussed further below. However, $Fe(II)_{HCl}$ and Fe_{ox1} remained more stable in summer, indicating a similar redox environment throughout the core profile. The lake water level rise induced a more reductive environment in sediments in summer, leading to a higher concentration of Fe(II) in both sediments and pore water (Figs. 3 and 5). The abundant Fe(II) consequently reacts with sulfide and results in higher concentrations of Fe_{AVS} in summer (Fig. 5).

Fe_{ox2} and Fe_{mag} remained more stable with depth in the PIZ core in both seasons although they exhibited a similar increase from winter to summer. However, the involvement of Fe_{ox2} and Fe_{mag} in the reductive dissolution cannot be ruled out. Firstly, the water level rise enhanced water mixing between lake water and pore water, leading to the deposition of suspended matter in sediments. The contents of total Fe and total Al in sediments subsequently increased significantly from winter to summer (Fig. 4). Therefore, the difference in concentration between different seasons cannot be used to judge whether they were reduced. The decline of SO_4^{2-} in pore water and increase of Fe(II) in pore water and sediments indicate a reductive environment, which is conductive to the reduction of Fe_{ox2} and Fe_{mag} (Herndon et al., 2018; Taylor and Konhauser, 2011). The reduction of crystalline ferric (oxyhydr)oxide minerals may occur via anaerobic oxidation of methane (Beal et al., 2009) or dissimilatory Fe reduction.

The overall trend of iron speciation in the SIZ core was basically similar with that in the PIZ core (Fig. 5). However, the sediment surface is exposed to air in winter, which results in low Fe (II) concentration in the upper 6 cm. The content of Fe-oxide minerals was relatively higher in SIZ than in PIZ, which is beneficial to P adsorption (Ajmal et al., 2018; Baken et al., 2015; Forsmann and Kjaergaard, 2014). In the upper 16 cm, Fe_{ox1} decreased significantly from winter to summer, indicating a reductive dissolution of reactive Fe minerals, which is consistent with the increase of $Fe(II)_{HCl}$ in sediments and Fe(II) in pore water. Associated with the reduction of SO_4^{2-} in pore water (Fig. 4), the increase of Fe_{AVS} can be predicted, which is consistent with the analyzed data. The bulk content of TFe and Al in the SIZ core remained basically the same in both seasons, suggesting that SIZ is less affected by the deposition of suspended matter. Under this scenario, no significant changes in Fe_{ox2} and Fe_{mag} content occur, and the water level rise can be ascertained to have little effect on these two Fe species.

Overall, the water level rise from winter to summer plays a crucial role in Fe cycling in sediments. Most notably, it changes the redox environment and leads to the transformation of $Fe(II)_{HCl}$ and Fe_{ox1}, which is a prominent feature of Fe cycling. Another major impact is that in the PIZ core, the enhanced water mixing between lake water and pore water induced the deposition of fine particles, which would change the bulk composition of sediments, such as TFe, Al, and organic matter. Moreover, the Fe speciation data indicate a significant difference between Dongting Lake and other euxinic oceans or lakes. The concentrations of Fe_{py} and Fe_{AVS} were very low (<1% of total Fe), suggesting that sulfates or sulfides are not very essential for Fe cycling in Dongting Lake as they are in other euxinic waters (Egger et al., 2015; Xiong et al., 2019), presumably because of the low TS and dissolved SO_4^{2-} contents.

4.3. Phosphorus cycling

4.3.1. Controls on P cycling throughout the cores

In winter, the decrease in Fe-P and Org-P over the top few centimeters in the PIZ core (Fig. 6) likely suggests the release of P from Fe-oxide dissolution during early diagenesis and organic matter degradation. Coupled with the peak dissolved P content in the sediment–water surface (Fig. 3), it might suggest diffusive loss of dissolved P to the overlying lake water. Although the Org-P profiles showed a clear increase below 18 cm, molar TOC/Org-P ratios (Fig. 7) provide evidence for extensive P mobilization during the degradation of organic matter. Molar TOC/Org-P ratios were considerably higher than the Redfield Ratio of

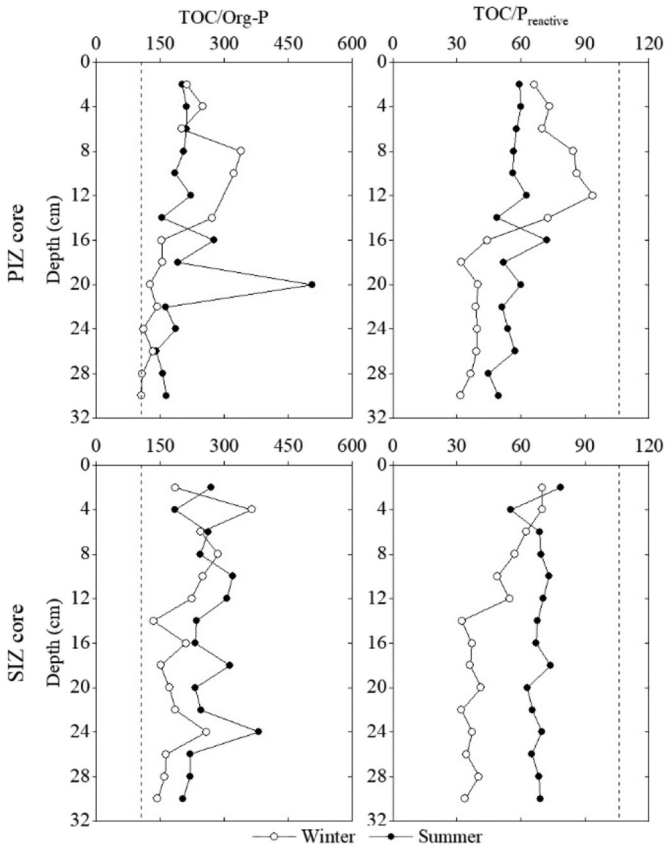

Fig. 7. Ratios of molar TOC/Org-P and TOC/$P_{reactive}$ profiles in the two cores. Dashed lines represent the Redfield TOC/P ratio (106:1).

106:1 (Fig. 7), which is consistent with the preferential recycling of P during organic matter degradation (Hupfer et al., 2004; Jilbert et al., 2011). However, the TOC/Org-P ratios decreased slightly and do not suggest preferential mobilization of phosphorus in sediments with depth, which is contrary to the general conclusions of preferential P remineralization. This abnormal phenomenon may be attributable to multiple factors, such as sediment compactness, moisture content, pH, temperature, bacterial biomass, and P content, which will affect the bacterial carbon–phosphorus lyase (Sosa et al., 2019; Zhang et al., 2019). Moreover, previous studies reported that autolytic phosphate recycling occurs very rapidly after the death of organisms without corresponding carbon release, thus explaining the high TOC/Org-P ratios of the top few centimeters of the PIZ core. For subsequent remineralization only less degradable P compounds are available and organic carbon is preferentially decomposed. Below these layers, the proportion of refractory TOC materials increase such that the decomposition rates of TOC and Org-P and the TOC/Org-P ratios of organic matter become equal (Balzer, 1984; Golterman, 1973; Krom and Berner, 1981). Consequently, the TOC/Org-P content decreases. This hypothesis is also supported by the similar changes of TOC content and the ratio of TOC/Org-P (Figs. 4, 7).

The P released from the degradation of organic matter might either be sequestered in the sediments as secondary phases or recycled back to the lake water. We examined molar TOC/$P_{reactive}$ ratios and found that the values are much lower than TOC/Org-P ratios, suggesting that most of the recycled organic P is sequestered in authigenic phases or sorbed to Fe-oxides (Anderson et al., 2001; Kraal et al., 2012). The TOC/$P_{reactive}$ ratios were also lower than the Redfield Ratio, likely suggesting the deposition of suspended particles, which can strongly adsorb dissolved P from the water column (Baken et al., 2016b; Withers and Jarvie, 2008).

The decrease of Fe-P induced by the reductive dissolution of Fe-oxides below 10 cm in the PIZ core, coupled with the significant Ca-P

decrease in winter (Fig. 7), is not conducive to the increase of adsorbed phosphorus and dissolved P in pore water (Figs. 6, 3). On the contrary, among all the P species, only Detr-P profiles showed sharp increases and a significant negative correlation with Fe-P and Ca-P at this depth, indicating that Fe-P and Ca-P were transformed into Detr-P. Studies have shown that P released by the reduction of Fe-oxides can be re adsorbed by $CaCO_3$, and carbon fluorapatite could potentially be converted to more crystalline apatite, which would be extracted as Detr-P, resulting in the increase of Detr-P (Kraal et al., 2017; Xiong et al., 2019).

With increasing depth, all P forms in the PIZ core were more stable in summer than in winter, while Fe-P and Org-P decreased slightly (Fig. 6). Although the total P in sediments was higher in summer than in winter, the similar distribution pattern of P speciation and TOC/P indicate that the mechanisms of P cycling throughout the core are similar in both seasons. However, the dissolved Fe and P in pore water increased considerably with depth, suggesting a more efficient reductive dissolution of Fe-oxides in summer (Fig. 3). The P concentration gradient also reflects the diffusion of dissolved P to the overlying lake water.

The main difference in phosphorus speciation between the SIZ and PIZ cores is that the contents of Fe-P and Ca-P are higher in the SIZ core than in the PIZ core, whereas Detr-P is lower in the SIZ core. Except for these differences, the variation patterns of bulk composition, and Fe and P speciation throughout the core were similar between SIZ and PIZ, likely indicating similar P cycling mechanisms in both cores. The mechanisms are mainly affected by the reductive dissolution of Fe-oxides, degradation of organic matter, and conversion between Ca-P and Detr-P.

4.3.2. Seasonal evolution of P

4.3.2.1. PIZ core. The seasonal evolution of phosphorus involves the mixing of pore water with the water column and the transformation of phosphorus speciation in sediments. In the PIZ core, with the lake water level rise, the entry of suspended particles into sediments with water flow increased the contents of TFe, Al, and TOC, further leading to the increase of Fe-P, Org-P, and TP (Fig. 6). This observation is further supported by the strong positive correlation between variations of TP and Fe-P, as well as TP and Org-P (Table 2). Specifically, the increase of TFe in sediments is consistent with the rise of iron (oxyhydr)oxides and ferrous minerals (Figs. 4, 5), which will lead to the adsorption of P and formation of ferrous phosphate minerals (vivianite). Moreover, the increase of TOC would directly result in the increase of Org-P.

Another prominent feature is that the increase of Org-P content is strongly correlated with those of Fe-P and Ex-P in the PIZ core (Table 2). These three P species appear to have similar sources. As discussed above, the water level rise would enhance the deposition of suspended particles, and the significant increase of TFe in sediments indicates a high proportion of Fe precipitates in the suspended particles. However, liberal P and organic matter have a strong tendency to adsorb on Fe precipitates or colloids (Baken et al., 2016a; Baken et al., 2016b; Gunnars et al., 2002; Van der Grift et al., 2018). Moreover, further coprecipitation occurs, leading to similar increases of these three P species. Fe-P and Ex-P exhibit a certain correlation ($R = 0.543$), which supports this view.

Table 2
Spearman correlation between variations in phosphorus speciation from winter to summer (*Correlation is significant at the 0.05 level (2-tailed); **Correlation is significant at the 0.01 level (2-tailed); Bold indicates a strong correlation ratio).

		Ex-P	Fe-P	Ca-P	Detr-P	Org-P	TP
PIZ core	Ex-P	1.000	0.543*	0.189	−0.357	**0.682****	0.354
	Fe-P		1.000	0.536*	**−0.775****	**0.789****	**0.793****
	Ca-P			1.000	**−0.754****	0.114	0.325
	Detr-P				1.000	−0.532*	−0.414
	Org-P					1.000	**0.768****
	TP						1.000
SIZ core	Ex-P	1.000	0.611*	0.493	−0.064	0.164	**0.668****
	Fe-P		1.000	**0.743****	−0.636*	0.339	**0.779****
	Ca-P			1.000	**−0.771****	0.182	**0.675****
	Detr-P				1.000	−0.389	−0.514*
	Org-P					1.000	**0.718****
	TP						1.000

The most remarkable difference in the P composition of sediments between winter and summer is that Detr-P sharply decreases while Ca-P considerably increases (Fig. 6). The relatively strong negative correlations between the variations of Detr-P and Ca-P, and also Detr-P and Fe-P suggest the conversion of Detr-P to Ca-P and Fe-P. Considering the relatively low total content and increment of Fe-P, most of the reduced Detr-P should transform to Ca-P. However, this appears unlikely because Detr-P is considered to be stable and resistant to the reaction. In this study, Detr-P was extracted by 10% HCl and considered to be composed mainly of detrital apatite of igneous or metamorphic origin (mainly fluorapatite, FAP) (Oxmann and Schwendenmann, 2014; Ruttenberg, 1992). Although FAP is relatively stable at the pH of most natural waters, experiments have showed that FAP can dissolve significantly under low pH (<4) (Guidry and Mackenzie, 2003). The low pH induced by H_2SO_4 produced by pyrite oxidation or respiration-related CO_2 in the vicinity of degrading organic matter can also lead to the acidic dissolution of detrital apatite (Filippelli, 2002; Gao et al., 2019; Kraal and Slomp, 2014). In the present study, the dissolution of detrital apatite should be induced by the degradation of organic matter, and this process would release HCO_3^-, PO_4^{3-}, and Ca^{2+} to pore water (Filippelli, 2002), which is consistent with the increase of HCO_3^-, P, and Ca^{2+} in pore water (Fig. 3). SI values of the two main carbonate minerals (calcite and dolomite, Fig. S4) increased considerably with depth in summer, suggesting the formation of authigenic carbonate minerals. Subsequently, coprecipitation or/and adsorption of phosphate with carbonate minerals occurred, resulting in the increase of Ca-P. Furthermore, the increased SI of hydroxyapatite (HAP) with depth in summer also indicates the formation of Ca-P.

To further examine the dissolution of detrital apatite and formation of authigenic Ca-P, we also applied inverse models. Pore water samples of the PIZ core (14 cm depth) were taken as an example considering the relatively comprehensive water chemical data covering both seasons. As discussed above, significant mixing of pore water and lake water occurs with the rise of lake water level. Accordingly, we set a mixture of pore water sample in winter and lake water in summer as initial water and pore water sample in summer as final water. The mixing ratio of pore water and lake water was based on Cl^- content. Mineralogical information involved in the model was derived from Huang et al. (2016) and Wen et al. (2016), and some potential reactants were added on the basis of discussions made in this study. Specifically, the degradation of organic matter induced by Fe(III) reduction and sulfate reduction was also added, and the processes can be described as follows (Larowe and Van Cappellen, 2011):

$$CH_2O + H_2O = CO_2 + 4H^+ + 4e^-$$

The results showed three reasonable models (Table 3) consistent with the mixing ratio between pore water in winter and lake water in summer (1.26:8.74). The models indicated conversion mechanisms from Detr-P to Ca-P and the dissolution of FAP promoting the formation of HAP, as shown in Models. These models clearly support the view that Detr-P transformed to Ca-P from winter to summer.

Except for Ca-P, the strong positive correlation between the variations in Fe-P and Detr-P indicate that a small portion of P released by FAP dissolution is absorbed by Fe minerals. Thus, the seasonal increase of Fe-P can be mainly attributed to two sources: one is the precipitation of suspended matter, and the other is P released by the dissolution of detrital apatite and then re-adsorbed by iron minerals. The increase of Fe-P is very similar to that of Fe_{ox1} (Figs. 5 and 6), indicating the

Table 3
Summary of mass transfer for selected inverse geochemical models (mmol). Negative values suggest precipitation, and positive values suggest dissolution.

Phase	Model-1	Model-2	Model-3	Stoichiometry
Albite	0.22	0.22	0.22	$NaAlSi_3O_8$
Calcite	−0.96	–	–	$CaCO_3$
Dolomite	0.59	0.59	0.59	$CaMg(CO_3)_2$
FeS(ppt)	–	–	−2.69	FeS
Fluorapatite	2.03	2.98	2.31	$Ca_5(PO_4)_3F$
Fluorite	−1.01	−1.49	−1.16	CaF_2
Goethite	0.03	0.03	2.72	FeOOH
Gypsum	3.15	2.67	2.34	$CaSO_4$
$H_2S(g)$	−3.51	−3.03	–	H_2S
Hydroxyapatite	−2.02	−2.98	−2.31	$Ca_5(PO_4)_3OH$
Kaolinite	−0.15	−0.15	−0.15	$Al_2Si_2O_5(OH)_4$
K-feldspar	0.09	0.09	0.09	$KAlSi_3O_8$
Quartz	−0.62	−0.62	−0.62	SiO_2
CH_2O	7.02	6.06	6.06	CH_2O

retention of most of the increased Fe-bound phosphorus on amorphous Fe-oxides. However, the gradual increase in dissolved Fe and P in pore water, coupled with the low SO_4^{2-} content (Fig. 3), provides a very suitable environment for the formation of Fe (II) phosphate (vivianite) (Egger et al., 2015; Rothe et al., 2016). The SI of vivianite increased progressively with depth, suggesting its potential formation (Fig. S4). Although vivianite content may be low and difficult to detect, its existence cannot be ignored.

4.3.2.2. SIZ core. The seasonal evolution of P was similar between the SIZ and PIZ cores. The relatively large correlation coefficients (Table 2) suggest that the increase of TP is mainly attributable to the increase in Fe-P and organic P. The increase of Ex-P and Ca-P also played an important role in the increase of TP, with correlation coefficients of 0.688 and 0.675 between TP and Ex-P, and TP and Ca-P, respectively. These findings collectively imply the coprecipitation of phosphate with Fe-oxides and calcite. The dissolution of detrital apatite also occurs and most of the released P is sequestered in authigenic phases. However, the increase of organic phosphorus did not show a significant positive correlation with Fe-P as in PIZ pores, indicating a different mechanism of organic P increase. Coupled with the higher DOC concentration in the water column and TOC in sediments in the SIZ core in summer, organic matter in SIZ can be inferred to mainly originate from the decomposition of herbaceous plants.

4.4. Implications for lake water quality protection

This study shows that suspended matter deposition associated with water level rise is an important source of phosphorus in sediments, and will increase the phosphorus load in sediments (Fig. 8). Phosphorus in the sediments will also be released to the overlying water through physical–chemical–biological processes, which can further increase the possibility of phosphorus pollution in Dongting Lake. With the intensification of agricultural activities, the phosphorus content in the soil around the lake will also increase significantly. Combined with the increasing frequency of extreme climate events, such as heavy rainfall, the water level rise will directly aggravate surface erosion, increase the possibility of the surrounding phosphorus rich soil entering the lake, and adversely affect the water quality of the lake.

Although this study has shed light on the conversion of Detr-P to Ca-P, the kinetic and thermodynamic characteristics remain unclear, and we hope to reveal these characteristics in future research.

5. Conclusions

We conducted the first detailed study of seasonal variations in the P cycle in a shallow freshwater lake, taking Dongting Lake as an example, which is significantly influenced by climate change and human activities. In an individual season, in both the permanent and seasonal inundation zones, the degradation of organic matter and reductive dissolution of Fe-oxides in the upper few centimeters of the sediment layer can release P to the pore water and also to the overlying water column. Below these layers, most of the released P is sequestered in authigenic phases and promote the formation of carbon fluorapatite, which could potentially convert to more crystalline apatite (Detr-P) (Fig. 8).

From winter to summer, the water level rises significantly, carrying abundant suspended matter rich in organic matter to the lake. In PIZ, the deposition of suspended matter increases the contents of Fe-bound P and organic P, which further increase total P. The rising water level also induces a more reductive environment at the lake bottom and enhances the reductive dissolution of Fe-oxides. However, in shallow lakes, sediments are in a relatively aerobic state, and the rapid decomposition of organic matter will release P from the sediment–water surface to the overlying water. Moreover, the aerobic degradation of organic matter can produce a large amount of CO_2, resulting in the decline of local pH and further dissolution and release of Detr-P. Subsequently, the released P is adsorbed or coprecipitated with calcium minerals,

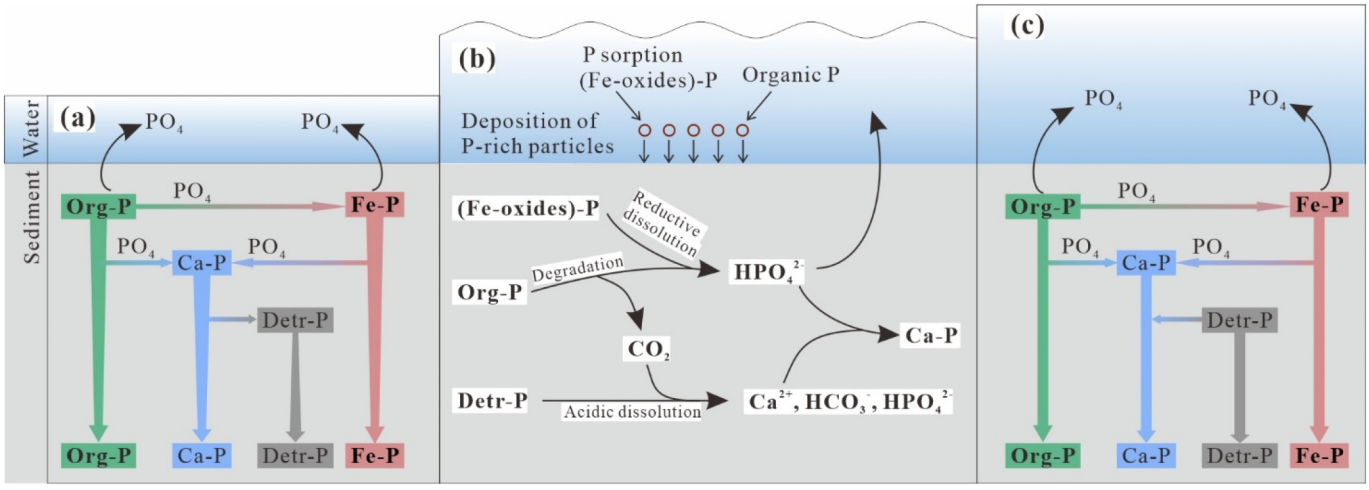

Fig. 8. Schematic overview of P cycling in Dongting Lake, taking PIZ as an example. Mechanisms of P cycling in (a) winter and (c) summer; gradients of the arrows indicate changes in contents, while the height of water column shows the water level. (b) Seasonal evolution mechanisms of P; the wave line indicates water level fluctuations from winter to summer.

resulting in the significant increase of Ca-P from winter to summer (Fig. 8). The mechanisms of phosphorus cycling are similar between SIZ and PIZ.

Therefore, the water level rise results in not only the increase of total P in sediments, but also the release of phosphorus adsorbed to oxides and the conversion of P from conservative speciation to active speciation. This P cycling pattern can enhance the risk of P release from sediments to the overlying water, posing strong risks to lake productivity and eutrophication.

CRediT authorship contribution statement

Xiancang Wu: Conceptualization, Data curation, Investigation, Methodology, Writing – original draft. **Teng Ma:** Conceptualization, Funding acquisition, Investigation, Methodology, Project administration, Writing – review & editing. **Yao Du:** Methodology, Writing – review & editing. **Qianqian Jiang:** Data curation, Investigation. **Shuai Shen:** Data curation, Investigation. **Wenhui Liu:** Data curation, Investigation.

Declaration of competing interest

The authors declare that they have no known competing financial interests or personal relationships that could have appeared to influence the work reported in this paper.

Acknowledgements

This work was funded by the National Natural Science Foundation of China (Nos. 41521001, 41630318), the Project of China Geological Survey (Nos. 2019040022, DD20190263, 12120100100015012l), and the Research Program for Geological Processes, Resources and Environment in the Yangtze River Basin (No. CUGCJ1702). The authors would like to thank all the reviewers who participated in the review and MJEditor (www.mjeditor.com) for its linguistic assistance during the preparation of this manuscript.

Appendix A. Supplementary data

Supplementary data to this article can be found online at https://doi.org/10.1016/j.scitotenv.2021.148383.

References

Ajmal, Z., Muhmood, A., Usman, M., Kizito, S., Lu, J., Dong, R., Wu, S., 2018. Phosphate removal from aqueous solution using iron oxides: adsorption, desorption and regeneration characteristics. J. Colloid Interface Sci. 528, 145–155.

Anderson, L., Delaney, M., Faul, K., 2001. Carbon to phosphorus ratios in sediments: implications for nutrient cycling. Glob. Biogeochem. Cy. 15 (1), 65–79.

Baken, S., Salaets, P., Desmet, N., Seuntjens, P., Vanlierde, E., Smolders, E., 2015. Oxidation of iron causes removal of phosphorus and arsenic from streamwater in groundwater-fed lowland catchments. Environ. Sci. Technol. 49 (5), 2886–2894.

Baken, S., Moens, C., van der Grift, B., Smolders, E., 2016a. Phosphate binding by natural iron-rich colloids in streams. Water Res. 98, 326–333.

Baken, S., Regelink, I.C., Comans, R.N.J., Smolders, E., Koopmans, G.F., 2016b. Iron-rich colloids as carriers of phosphorus in streams: a field-flow fractionation study. Water Res. 99, 83–90.

Balzer, W., 1984. Organic matter degradation and biogenic element cycling in a nearshore sediment (Kiel Bight). Limnol. Oceanogr. 29 (6), 1231–1246.

Beal, E.J., House, C.H., Orphan, V.J., 2009. Manganese-and iron-dependent marine methane oxidation. Science 325 (5937), 184–187.

Burton, E.D., Sullivan, L.A., Bush, R.T., Johnston, S.G., Keene, A.F., 2008. A simple and inexpensive chromium-reducible sulfur method for acid-sulfate soils. Appl. Geochem. 23 (9), 2759–2766.

Canfield, D.E., 1989. Reactive iron in marine sediments. Geochim. Cosmochim. Acta 53 (3), 619–632.

Canfield, D.E., Raiswell, R., Westrich, J.T., Reaves, C.M., Berner, R.A., 1986. The use of chromium reduction in the analysis of reduced inorganic sulfur in sediments and shales. Chem. Geol. 54, 149–155.

Carmignani, J.R., Roy, A.H., 2017. Ecological impacts of winter water level drawdowns on lake littoral zones: a review. Aquat. Sci. 79 (4), 803–824.

Chen, X., Mcgowan, S., Xu, L., Zeng, L., Yang, X., 2016. Effects of hydrological regulation and anthropogenic pollutants on Dongting Lake in the Yangtze floodplain. Ecohydrology 9 (2), 315–325.

Coppens, J., Özen, A., Tavşanoğlu, Ü.N., Erdoğan, Ş., Levi, E.E., Yozgatlıgil, C., Jeppesen, E., Beklioğlu, M., 2016. Impact of alternating wet and dry periods on long-term seasonal phosphorus and nitrogen budgets of two shallow Mediterranean lakes. Sci. Total Environ. 563, 456–467.

Cui, G., Su, X., Liu, Y., Zheng, S., 2021. Effect of riverbed sediment flushing and clogging on river-water infiltration rate: a case study in the Second Songhua River, Northeast China. Hydrogeol. J. 29 (2), 551–565.

Dijkstra, N., Kraal, P., Séguret, M.J.M., Flores, M.R., Gonzalez, S., Rijkenberg, M.J.A., Slomp, C.P., 2018. Phosphorus dynamics in and below the redoxcline in the Black Sea and implications for phosphorus burial. Geochim. Cosmochim. Acta 222, 685–703.

Du, Y., Cai, S., Zhang, X., Zhao, Y., 2001. Interpretation of the environmental change of Dongting Lake, middle reach of Yangtze River, China, by 210Pb measurement and satellite image analysis. Geomorphology 41 (2–3), 171–181.

Egger, M., Jilbert, T., Behrends, T., Rivard, C., Slomp, C.P., 2015. Vivianite is a major sink for phosphorus in methanogenic coastal surface sediments. Geochim. Cosmochim. Acta 169, 217–235.

Feng, L., Hu, C., Chen, X., Zhao, X., 2013. Dramatic inundation changes of China's two largest freshwater lakes linked to the Three Gorges Dam. Environ. Sci. Technol. 47 (17), 9628–9634.

Filippelli, G.M., 2002. The global phosphorus cycle. Rev. Mineral. Geochem. 48 (1), 391–425.

Flores-Alsina, X., Solon, K., Kazadi Mbamba, C., Tait, S., Gernaey, K.V., Jeppsson, U., Batstone, D.J., 2016. Modelling phosphorus (P), sulfur (S) and iron (Fe) interactions for dynamic simulations of anaerobic digestion processes. Water Res. 95, 370–382.

Forsmann, D.M., Kjaergaard, C., 2014. Phosphorus release from anaerobic peat soils during convective discharge — effect of soil Fe:P molar ratio and preferential flow. Geoderma 223–225, 21–32.

Gachter, R., Muller, B., 2003. Why the phosphorus retention of lakes does not necessarily depend on the oxygen supply to their sediment surface. Limnol. Oceanogr. 48 (2), 929–933.

Gao, C., Sander, M., Agethen, S., Knorr, K.-H., 2019. Electron accepting capacity of dissolved and particulate organic matter control CO_2 and CH_4 formation in peat soils. Geochim. Cosmochim. Acta 245, 266–277.

Goldberg, T., Archer, C., Vance, D., Thamdrup, B., McAnena, A., Poulton, S.W., 2012. Controls on Mo isotope fractionations in a Mn-rich anoxic marine sediment, Gullmar Fjord, Sweden. Chem. Geol. 296-297, 73–82.

Golterman, H., 1973. Vertical movement of phosphate in freshwater. Environmental Phosphorus Handbook.

Guidry, M.W., Mackenzie, F.T., 2003. Experimental study of igneous and sedimentary apatite dissolution. Geochim. Cosmochim. Acta 67 (16), 2949–2963.

Gunnars, A., Blomqvist, S., Johansson, P., Andersson, C., 2002. Formation of Fe (III) oxyhydroxide colloids in freshwater and brackish seawater, with incorporation of phosphate and calcium. Geochim. Cosmochim. Acta 66 (5), 745–758.

Hambright, K.D., Eckert, W., Leavitt, P.R., Schelske, C.L., 2004. Effects of historical lake level and land use on sediment and phosphorus accumulation rates in Lake Kinneret. Environ. Sci. Technol. 38 (24), 6460–6467.

Herndon, E.M., Havig, J.R., Singer, D.M., McCormick, M.L., Kump, L.R., 2018. Manganese and iron geochemistry in sediments underlying the redox-stratified Fayetteville Green Lake. Geochim. Cosmochim. Acta 231, 50–63.

House, W.A., 2003. Geochemical cycling of phosphorus in rivers. Appl. Geochem. 18 (5), 739–748.

Hu, T., Mao, J., Pan, S., Dai, L., Zhang, P., Xu, D., Dai, H., 2018. Water level management of lakes connected to regulated rivers: an integrated modeling and analytical methodology. J. Hydrol. 562, 796–808.

Huang, W., Zheng, B., Jiang, X., 2016. Effect of ionic strength on phosphorus removal with modified sediments in lake: kinetics and equilibrium studies. Int. J. Electrochem. Sci. 11, 9972.

Hupfer, M., Ruübe, B., Schmieder, P., 2004. Origin and diagenesis of polyphosphate in lake sediments: a 31P‡NMR study. Limnol. Oceanogr. 49 (1), 1–10.

Jilbert, T., Slomp, C., Gustafsson, B.G., Boer, W., 2011. Beyond the Fe-P-redox connection: preferential regeneration of phosphorus from organic matter as a key control on Baltic Sea nutrient cycles. Biogeosciences 8 (6), 1699–1720.

Kraal, P., Slomp, C.P., 2014. Rapid and extensive alteration of phosphorus speciation during oxic storage of wet sediment samples. PLoS One 9 (5), e96859.

Kraal, P., Slomp, C.P., de Lange, G.J., 2010. Sedimentary organic carbon to phosphorus ratios as a redox proxy in Quaternary records from the Mediterranean. Chem. Geol. 277 (1–2), 167–177.

Kraal, P., Slomp, C., Reed, D., Reichart, G.-J., Poulton, S., 2012. Sedimentary phosphorus and iron cycling in and below the oxygen minimum zone of the northern Arabian Sea. Biogeosciences 9 (7), 2603–2624.

Kraal, P., Bostick, B.C., Behrends, T., Reichart, G.-J., Slomp, C.P., 2015. Characterization of phosphorus species in sediments from the Arabian Sea oxygen minimum zone: combining sequential extractions and X-ray spectroscopy. Mar. Chem. 168, 1–8.

Kraal, P., Dijkstra, N., Behrends, T., Slomp, C.P., 2017. Phosphorus burial in sediments of the sulfidic deep Black Sea: key roles for adsorption by calcium carbonate and apatite authigenesis. Geochim. Cosmochim. Acta 204, 140–158.

Krom, M.D., Berner, R.A., 1981. The diagenesis of phosphorus in a nearshore marine sediment. Geochim. Cosmochim. Acta 45 (2), 207–216.

LaRowe, D.E., Van Cappellen, P., 2011. Degradation of natural organic matter: a thermodynamic analysis. Geochim. Cosmochim. Acta 75 (8), 2030–2042.

Lécrivain, N., Clément, B., Dabrin, A., Seigle-Ferrand, J., Bouffard, D., Naffrechoux, E., Frossard, V., 2021. Water-level fluctuation enhances sediment and trace metal mobility in lake littoral. Chemosphere 264, 128451.

Li, J., Zhang, Y., Katsev, S., 2018. Phosphorus recycling in deeply oxygenated sediments in Lake Superior controlled by organic matter mineralization. Limnol. Oceanogr. 63 (3), 1372–1385.
Liang, T., Tong, Y., Wang, X., Wang, L., 2017. Release of reactive phosphorus from sediments in Dongting Lake linked with the Yangtze River. Environ. Chem. 14 (1), 48–54.
Markovic, S., Liang, A., Watson, S.B., Guo, J., Mugalingam, S., Arhonditsis, G., Morley, A., Dittrich, M., 2019. Biogeochemical mechanisms controlling phosphorus diagenesis and internal loading in a remediated hard water eutrophic embayment. Chem. Geol. 514, 122–137.
McMahon, K.D., Read, E.K., 2013. Microbial contributions to phosphorus cycling in eutrophic lakes and wastewater. Annu. Rev. Microbiol. 67 (1), 199–219.
Nivala, J., Knowles, P., Dotro, G., García, J., Wallace, S., 2012. Clogging in subsurface-flow treatment wetlands: measurement, modeling and management. Water Res. 46 (6), 1625–1640.
O'Connell, D.W., Mark Jensen, M., Jakobsen, R., Thamdrup, B., Joest Andersen, T., Kovacs, A., Bruun Hansen, H.C., 2015. Vivianite formation and its role in phosphorus retention in Lake Ørn, Denmark. Chem. Geol. 409, 42–53.
Oxmann, J.F., Schwendenmann, L., 2014. Quantification of octacalcium phosphate, authigenic apatite and detrital apatite in coastal sediments using differential dissolution and standard addition. Ocean Sci. 10 (3), 571–585.
Poulton, S.W., Canfield, D.E., 2005. Development of a sequential extraction procedure for iron: implications for iron partitioning in continentally derived particulates. Chem. Geol. 214 (3–4), 209–221.
Poulton, S.W., Krom, M.D., Raiswell, R., 2004. A revised scheme for the reactivity of iron (oxyhydr) oxide minerals towards dissolved sulfide. Geochim. Cosmochim. Acta 68 (18), 3703–3715.
Reddy, K.R., Kadlec, R.H., Flaig, E., Gale, P.M., 1999. Phosphorus retention in streams and wetlands: a review. Crit. Rev. Environ. Sci. Technol. 29 (1), 83–146.
Ren, Z., Qu, X., Zhang, M., Yu, Y., Peng, W., 2019. Distinct bacterial communities in wet and dry seasons during a seasonal water level fluctuation in the largest freshwater lake (Poyang Lake) in China. Front. Microbiol. 10, 1167.
Rothe, M., Frederichs, T., Eder, M., Kleeberg, A., Hupfer, M., 2014. Evidence for vivianite formation and its contribution to long-term phosphorus retention in a recent lake sediment: a novel analytical approach. Biogeosciences 11 (18), 5169–5180.
Rothe, M., Kleeberg, A., Hupfer, M., 2016. The occurrence, identification and environmental relevance of vivianite in waterlogged soils and aquatic sediments. Earth-Sci. Rev. 158, 51–64.
Ruttenberg, K.C., 1992. Development of a sequential extraction method for different forms of phosphorus in marine sediments. Limnol. Oceanogr. 37 (7), 1460–1482.
Schenau, S., Slomp, C., De Lange, G., 2000. Phosphogenesis and active phosphorite formation in sediments from the Arabian Sea oxygen minimum zone. Mar. Geol. 169 (1–2), 1–20.
Slomp, C.P., Gaast, S., Raaphorst, W.V., 1996. Phosphorus binding by poorly crystalline iron oxides in North Sea sediments. Mar. Chem. 52 (1), 55–73.
Sosa, O.A., Repeta, D.J., DeLong, E.F., Ashkezari, M.D., Karl, D.M., 2019. Phosphate-limited ocean regions select for bacterial populations enriched in the carbon–phosphorus lyase pathway for phosphonate degradation. Environ. Microbiol. 21 (7), 2402–2414.
Stookey, L.L., 1970. Ferrozine-a new spectrophotometric reagent for iron. Anal. Chem. 42 (7), 779–781.
Su, X., Cui, G., Wang, H., Dai, Z., Woo, N.-C., Yuan, W., 2018. Biogeochemical zonation of sulfur during the discharge of groundwater to lake in desert plateau (Dakebo Lake, NW China). Environ. Geochem. Health 40 (3), 1051–1066.
Tang, X., Wu, M., Li, R., 2018. Phosphorus distribution and bioavailability dynamics in the mainstream water and surface sediment of the Three Gorges Reservoir between 2003 and 2010. Water Res. 145, 321–331.
Tao, Y., Deng, Y., Du, Y., Xu, Y., Leng, Z., Ma, T., Wang, Y., 2020. Sources and enrichment of phosphorus in groundwater of the Central Yangtze River Basin. Sci. Total Environ. 737, 139837.
Taylor, K.G., Konhauser, K.O., 2011. Iron in earth surface systems: a major player in chemical and biological processes. Elements 7 (2), 83–88.
Tian, Z., Zheng, B., Wang, L., Li, H., Wang, X., 2017. Effects of river-lake interactions in water and sediment on phosphorus in Dongting Lake, China. Environ. Sci. Pollut. R. 24 (29), 23250–23260.
Ulrich, C., Hubbard, S.S., Florsheim, J., Rosenberry, D., Borglin, S., Trotta, M., Seymour, D., 2015. Riverbed clogging associated with a California riverbank filtration system: an assessment of mechanisms and monitoring approaches. J. Hydrol. 529, 1740–1753.
Van der Grift, B., Oste, L., Schot, P., Kratz, A., van Popta, E., Wassen, M., Griffioen, J., 2018. Forms of phosphorus in suspended particulate matter in agriculture-dominated lowland catchments: Iron as phosphorus carrier. Sci. Total Environ. 631–632, 115–129.
Vanderkelen, I., van Lipzig, N.P.M., Thiery, W., 2018. Modelling the water balance of Lake Victoria (East Africa) – part 1: observational analysis. Hydrol. Earth Syst. Sci. 22 (10), 5509–5525.
Wen, J., Yi, Y., Zeng, G., 2016. Effects of modified zeolite on the removal and stabilization of heavy metals in contaminated lake sediment using BCR sequential extraction. J. Environ. Manag. 178, 63–69.
Withers, P.J., Jarvie, H.P., 2008. Delivery and cycling of phosphorus in rivers: a review. Sci. Total Environ. 400 (1–3), 379–395.
Wu, X., Li, C., Sun, B., Geng, F., Gao, S., Lv, M., Ma, X., Li, H., Xing, L., 2020a. Groundwater hydrogeochemical formation and evolution in a karst aquifer system affected by anthropogenic impacts. Environ. Geochem. Health 42 (9), 2609–2626.
Wu, X., Ma, T., Wang, Y., 2020b. Surface water and groundwater interactions in wetlands. J. Earth Sci.-China 31 (5), 1016–1028.
Xiong, Y., Guilbaud, R., Peacock, C.L., Cox, R.P., Canfield, D.E., Krom, M.D., Poulton, S.W., 2019. Phosphorus cycling in Lake Cadagno, Switzerland: a low sulfate euxinic ocean analogue. Geochim. Cosmochim. Acta 251, 116–135.
Ye, X., Zhang, Q., Liu, J., Li, X., Xu, C.-y., 2013. Distinguishing the relative impacts of climate change and human activities on variation of streamflow in the Poyang Lake catchment, China. J. Hydrol. 494, 83–95.
Yu, Y., Mei, X., Dai, Z., Gao, J., Li, J., Wang, J., Lou, Y., 2018. Hydromorphological processes of Dongting Lake in China between 1951 and 2014. J. Hydrol. 562, 254–266.
Yuan, Y., Zeng, G., Liang, J., Huang, L., Hua, S., Li, F., Zhu, Y., Wu, H., Liu, J., He, X., He, Y., 2015. Variation of water level in Dongting Lake over a 50-year period: implications for the impacts of anthropogenic and climatic factors. J. Hydrol. 525, 450–456.
Yuan, R., Wang, M., Wang, S., Song, X., 2020. Water transfer imposes hydrochemical impacts on groundwater by altering the interaction of groundwater and surface water. J. Hydrol. 583, 124617.
Zhang, J.-Z., Guo, L., Fischer, C.J., 2010. Abundance and chemical speciation of phosphorus in sediments of the Mackenzie River Delta, the Chukchi Sea and the Bering Sea: importance of detrital apatite. Aquat. Geochem. 16 (3), 353–371.
Zhang, Z.-c., Hou, G., Liu, M., Wei, T.-x., Sun, J., 2019. Degradation induces changes in the soil C:N:P stoichiometry of alpine steppe on the Tibetan Plateau. J. Mt. Sci.-Engl. 16 (10), 2348–2360.
Zheng, Z., Li, Y., Guo, Y., Xu, Y., Liu, G., Du, C., 2015. Landsat-based long-term monitoring of total suspended matter concentration pattern change in the wet season for Dongting Lake, China. Remote Sens-Basel 7 (10), 13975–13999.
Zhu, G., Yang, Y., 2018. Variation laws and release characteristics of phosphorus on surface sediment of Dongting Lake. Environ. Sci. Pollut. R. 25 (13), 12342–12351.